Russian Journal of Herpetology Vol. 28, No. 5, 2021, pp. 281 – 290

DOI: 10.30906/1026-2296-2021-28-5-281-290

SEROUS GLANDS IN THE SKIN OF THE TUNGARA FROG, *Engystomops pustulosus* (COPE, 1864) (ANURA, LEPTODACTYLIDAE): DEGENERATED SECRETORY UNITS ARE SELECTIVELY REMOVED BY MACROPHAGES

Irina Arifulova,[1] Giovanni Delfino,[2]* Tatjana Dujsebayeva,[1] Galina Fedotovskikh,[3] and Filippo Giachi[2]

Submitted February 5, 2021

The cutaneous apparatus of *Engystomops pustulosus* (Cope, 1864) (the Tungara frog) includes serous glands that show impressive patterns of degeneration in their syncytial secretory units, and thus represent suitable organ models to investigate the role of macrophages in renewal processes of multicellular structures. The present case report exploits this chance and highlights that: (a) degenerating glands pertain to the Ia line of the polymorphic serous gland assortment in Tungara skin; (b) resident macrophages migrate from spongy dermis and remove syncytium debris; (c) secretory syncytium collapse results from impairment of the equilibrium between serous product manufacturing/storage and merocrine release into the dermal environment; (d) Intercalated tract (or gland neck) and myoepithelium (included its ortho-sympathetic nerve supply), are neither involved in degeneration nor affected by macrophage response. According to present evidence and current literature, it is concluded that the scavenger activity of macrophages prepares secretory unit renewal, performed by stem cells from the neck. In addition, gland functional rehabilitation may rely on effectiveness of the preexisting neuromuscular apparatus to achieve secretory bulk release onto the cutaneous surface.

Keywords: Tungara frog; dermal macrophages; serous glands; ultrastructure.

INTRODUCTION

Dorsal skin of the leptodactylid frog *Engystomops pustulosus* (the Tungara) exhibits a noticeably polymorphic gland arsenal of the serous type (Delfino et al., 2015). It includes type Ia and II glands in the outer spongy dermis, as well as type Ib glands, which extend in depth to the compact dermis with their large secretory units. These glands produce, respectively: granules of heterogeneous morphology and variable electron-density, encircled by wide halos; light secretory vesicles; and granules without halos, with consistent morphology and remarkable density. Differences between serous products are consistent with functional traits that emphasize their specific features during the storage within secretory unit cytoplasm. Type Ia and Ib granules keep peculiar relationships with the cytoplasm, which protrudes towards them through typical arrays of numerous thin microvilli and, respectively, few large outgrowths. Type II vesicles contain finely dispersed products with a variable density that becomes homogeneous after sequential merging processes. In addition to such outstanding gland polymorphism, the outer spongy dermis of Tungara contains structureless secretory units devoid of any product, which have been related to exhausted serous glands.

In anuran serous glands, the variety of features of secretory products is fashioned during the long-lasting phase of intracytoplasmic product maturation (Delfino et al., 2014). Maturation progresses from Golgi areas in the periphery of syncytial secretory units, according to a centripetal gradient of wide range of substructural traits (Melzer et al., 2013). In anuran cutaneous glands, the syncytial structure is a suitable alternative to the epithelial arrangement, when fast intracellular signaling is

[1] Laboratory of Ornithology and Herpetology, Institute of Zoology of the Republic of Kazakhstan, al-Farabi prosp., 93, Almaty 050060, Kazakhstan.

[2] Dipartimento di Biologia, Università degli Studi Di Firenze, via La Pira 4, Florence, I-50121, Italy; e-mail: giovanni.delfino@unifi.it

[3] Department of Pathomorphology, National Scientific Medical Center, Abylai Khan prosp., 42, Nur-Sultan 020000, Kazakhstan.

* Corresponding author.

needed to coordinate synthesis and post-Golgi processing of large amounts of products (Delfino et al., 1988), which include cytotoxins (Balboni et al., 1992; Sanna et al., 1993) along with paracrine, regulative molecules (Quagliata et al., 2008a). On the other hand, intracytoplasmic maturation causes irreversible subcellular change: organelles decrease in number, and become restricted in an electron-opaque peripheral cytoplasm containing a single row of nuclei. Meanwhile, the wide central cytoplasm that stores secretory products becomes electron-translucent, and the sharp contrast between the peripheral and central, zones (Delfino et al., 2002) gives the false impression of a real lumen holding secretory products (Delfino et al., 2014). Actually, anurans have developed a successful intracytoplasmic packaging of cytotoxic compounds, as an advanced adaption of the chemical skin defense performed by serous glands. Secretory granules are, indeed, active organelles, which reduce cytoplasm damage by maintaining noxious molecules in a suitable aggregation phase. Such structural steadiness is achieved through a fine tuning of the chemical and physical conditions that influence their membrane-bounded microenvironment (Nosi et al., 2013).

Occurrence of degenerated serous units in Tungara provides the opportunity of studying the severe effects of impairment of the mechanisms regulating intracytoplasmic storage of noxious molecules in cutaneous glands, as well as the response of skin to gland damage. The present case report exploits the chance of increasing ultrastructural knowledge of these fundamental themes dealing with the functional morphology of anuran skin. In detail, this account aims at: (a) identifying type/s of serous glands involved in degenerative processes; (b) describing the ultrastructural traits of the clearance activity of resident dermal macrophages towards glands with exhausted secretory units; and (c) recognizing the possible causes of gland collapse. Furthermore, (d) the study extends investigation to other gland components, namely intercalated tract (or neck) and myoepithelium, in order to ascertain their possible roles in integral gland rehabilitation.

MATERIAL AND METHODS

Skin samples analysed in the present case report belong to a specimen from the pool investigated in a previous study (Delfino et al., 2015). In detail, strips (9 – 16 cm^2 surface area) were removed from the dorsal skin, which contains large collection of serous glands, and treated, 2 h, 4°C, with fixative of Karnovsky (1965). This is an aldehyde solution, prepared in the 1 M, pH 7.0 buffer cacodylate, also used in the following steps of sample rinsing and osmication. Once rinsed, skin strips were reduced in size and post-fixed with 1% OsO_4 (90 min, 4°C), washed in the buffer, dehydrated with ethanol, soaked in propylene oxide, and embedded in Epon 812, to obtain flat blocks after polymerization. For Light Microscopy (LM) investigations, 1.5 μm thick sections were obtained using glass knives on an 8800 ULTROTOME III LKB. These semithin sections were stained with toluidine blue (1% in borax buffered solution), and studied with a LEITZ DMRB, which allowed collecting digital images (JPG) and preparing TEM observations. For this purpose, ultrathin sections (silver grey to gold yellow, interferential colours) were obtained with an ULTROTOME NOVA LKB, equipped with a DIATOME knife, and were collected on 200 – 300 mesh, uncoated copper grids. Ultrathin sections were electron-dense stained with a hydroalcoholic, saturated solution of uranyl acetate (25 mg/ml), followed by 2 mg/ml alkaline lead citrate, and observed (80 KV) with a PHILIPS 201 TEM (BIO, UNIFI), to collect images on fine grain release, 35-mm films. Finally, these analog negatives were acquired and stored as TIFF or PSD files through a DIMAGE SCAN DUAL (MINOLTA).

RESULTS

LM Observations

Glands with secretory units undergoing degeneration were detected along with active serous and mucous glands in the outer (closely sub-epidermal) spongy dermis of skin areas that did not show any evidence of damage (Fig. 1). Degenerating secretory units were ellipsoidal in shape, with sizes comparable to type Ia serous units (major axis ranging 90 – 120 μm), and smaller than type Ib units (600 – 700 μm). Therefore, only upper portions of such elongated units were detectable in the outer spongy dermis (Fig. 1C). In intermediate stages of degeneration, secretory units displayed weakly stained syncytia, which were almost empty and only contained scanty, minute vesicles with light compartments (Fig. 1A). Roundish peripheral nuclei of the syncytium were still recognizable, although some underwent massive (bulk) engulfing by macrophages that were closely interposed between them (Fig. 1A), as stressed by peripheral sections of the secretory unit (Fig. 1B). Increasing degeneration of secretory syncytia led to discrete regions with differential densities of cytoplasm, bounded by fissures originated by breakdown processes (Fig. 1C). Macrophages crossed the thin discontinuous myoepithelium and moved towards the centre of the secretory unit through such pathway of interstices in the decaying syncytium (Fig. 1C). This continuous inflow of migrating

cells was accompanied by total loss of syncytial cytoplasm, which led to the impressive patterns typical of the ultimate stage of degeneration: glands were just reduced to their myoepithelial envelops, while the compartments of the former secretory units held collections of macrophages suspended in a fluid medium (Fig. 1D).

TEM Observations

For convenience, ultrastructural investigations were performed according to a staging based on the above LM features, namely referring to intermediate and, respectively, ultimate stages of degeneration.

Glands in intermediated stages of degeneration. The massive macrophage transit towards the secretory syncytium possibly induced local and slight contractile responses in myoepithelial cells, as suggested by the electron-dense myofilament apparatus in sarcoplasm, and prominent arrays of thickened hemidesmosome-like junctions on the dermal side of sarcolemma (Fig. 2A). Low magnification images of degenerating syncytia disclosed heterogeneous cytoplasm backgrounds, due to alternating areas with different densities (Fig. 2A, B). Apparently, these differential features indicated variable degrees of hyaloplasm coagulation, which led to finely grained condensation (Fig. 2C – E). Secretory syncytia maintained a periphery-centre, functional polarization, with nuclei at the secretory unit-myoepithelium interface (Fig. 2A, C). The peripheral nuclei exhibited incipient patterns of pyknosis, as revealed by clumping of chromatin and thinning of karyoplasm (Fig. 2C). Zones of hyaloplasm with variable electron-opacity did not exhibit definite outlines in section, but secretory residues had distinct profiles, since maintained a limiting membrane (Fig. 2A, B). These vestigial secretory granules consisted of rarefied material or exhibited empty compartments (Fig. 2B), and were engaged in merging processes with small vesicles carrying electron-opaque products (Fig. 2D). Further vesicle-like structures, bounded by intact limiting membranes, contained inner networks of ramified electron-opaque rodlets, usually crowded at a pole (Fig. 2D, E). These minute sticks arose from the syncytium encircling the vesicles (Fig. 2E) in the shape of thin microvilli, and were characterized by a dense cytoplasm that contained single tubules with a thick wall (Fig. 2F).

Peripheral regions of secretory syncytium held macrophages exhibiting a variety of morphological traits, showing sequential activities of their constitutive role: migration, phagocytosis, and intracytoplasmic processing of cytoplasmic waste. Migrating macrophages displayed an irregular shape, with cell processes (pseudopodia) that fitted the labyrinthine path of breakdown interstices (Fig. 3A). Their nuclei were deeply lobed (Fig. 3B), and cytoplasm contained scattered organelles: flat complements of the rough endoplasmic reticulum (rer, Fig. 3C); scanty tubules of the smooth endoplasmic reticulum (ser, Fig. 3B); mitochondria with moderately electron-dense matrix and elongated, longitudinal cristae (Fig. 3D); and the typical machinery of primary lysosomes, characterized by low to high density contents (Fig. 3B – D). Phagocytizing macrophages exhibited

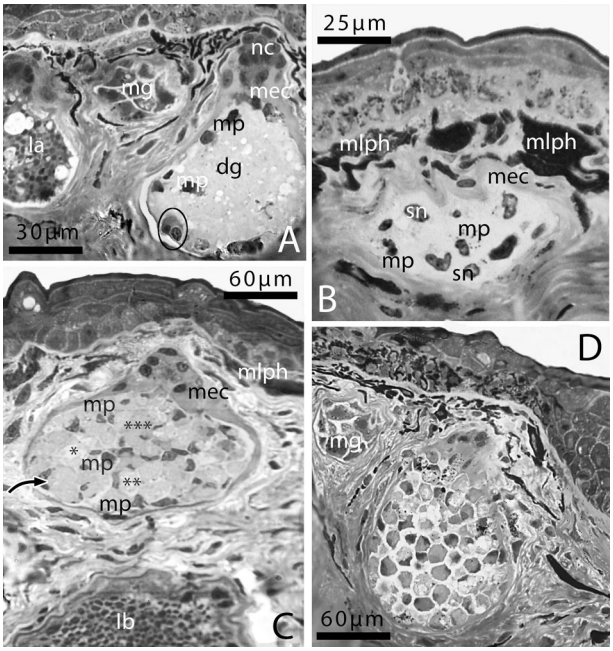

Fig. 1. LM features of glands in intermediate (**A – C**) and ultimate (**D**) stages of degeneration. Beside providing a possible sequence of decay steps, the figure shows components of the microenvironment of the degenerating secretory units: healthy glands, epidermis and spongy dermis, which exhibit unchanged features. Notice that the major axis of degenerating glands may be oriented orthogonal (**A**, **D**) or parallel (**B**, **C**) to epidermis: **A**, contiguous type Ia, mucous (mg) and degenerating (dg) glands. The secretory unit in intermediate stage of degeneration contains peripheral macrophages (mp), involved in phagocytosis of secretory syncytium debris, including nuclei (compare the selected area with Figs. 2A, C, 4B). Numerous stem cells (nc) are stacked in the gland intercalated tract, or neck, where myoepithelial cells (mec) converge; **B**, as an effect of this peripheral (quasi-tangential) section, macrophages (mp) and residual nuclei (sn) appear in the center of syncytium. Melanophores (mlph) are prominent cells in the spongy dermis; mec, myoepithelial cell; **C**, Degenerating syncytium exhibits discrete portions with different cytoplasm densities (*, **, ***), separated by fissures that allow movement of macrophages (mp) towards the center. Arrow points to a gap between myoepithelial cells. The lower third of this panel shows the upper portion of a type Ib gland that deepens into the inner layers of spongy dermis with its elongated secretory unit; mec, myoepithelial cell; mlph, melanophore; **D**, this fully exhausted gland, which lost its secretory syncytium entirely, exhibits an inner empty space containing large collection of scavenger macrophages, with prevailing polyhedral shapes; mg, mucous gland.

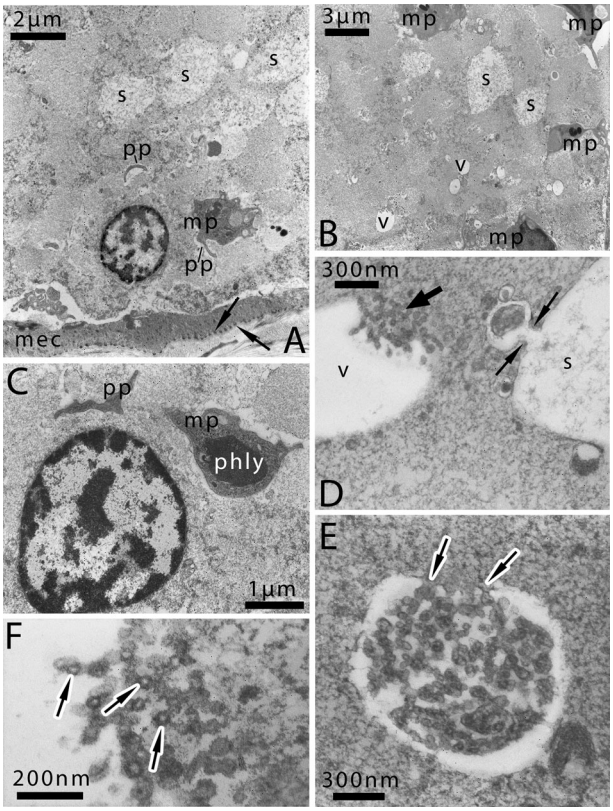

Fig. 2. TEM features of secretory syncytia in intermediate stages of degeneration: residual patterns of product maturation suggest that degenerating glands pertain to the serous Ia line. The figure also discloses emergent features of nuclear damage which contrast with advanced patterns of cytoplasm decay in the syncytium. Panels A and C show bulk phagocytosis involving a syncytial nucleus (compare with Figs. 1A and 4B): **A**, representative patterns of gland periphery, including: a syncytial nucleus, a macrophage (mp, see Fig. 3F for details), residual secretory granules (s), and cytoplasm with variable density areas. Notice cytoplasm processes (pseudopodia, pp), emerging from the macrophage. Also note thickened hemidesmosome-like junctions (arrows) in the slightly contracted mec; **B**, gland periphery: polymorphic macrophages (mp), empty vesicles (v), and residual secretory granules (s); **C**, this laminar pseudopodium (pp) approaches the residual nucleus characterized by slight patterns of pycnosis. The macrophage (mp) contains a secondary lysosome (or phagolysosome, phly) produced by previous phagocytosis processes; **D**, vestigial patterns of serous product processing: minute vesicles merge (arrows) with the membrane encircling a residual secretory granule (s), contiguous to a wider vesicle (v) that contains a thick network of dense rodlets (large arrow); **E**, peripheral section of a vesicle, showing that these rodlets originate from the cytoplasm (arrows); **F**, this detail of panel D discloses minute channels inside rodlets (arrows).

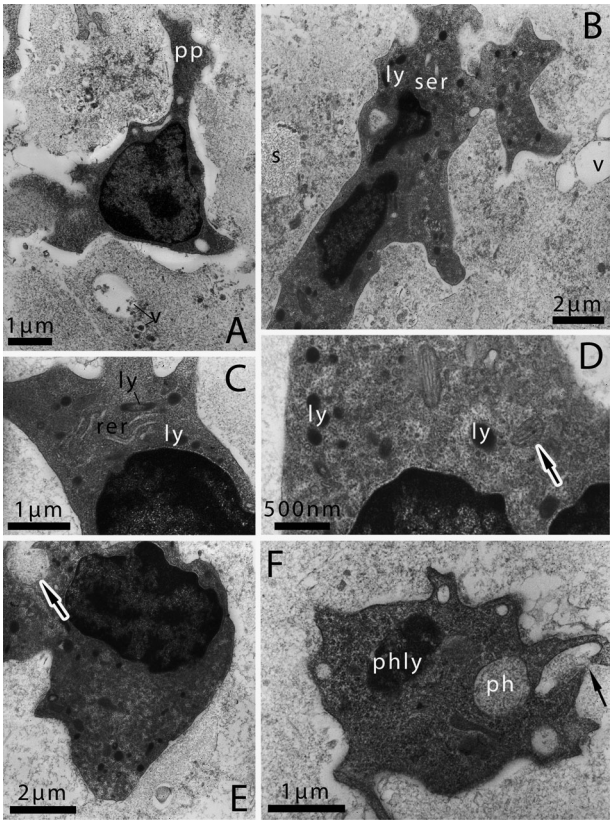

Fig. 3. TEM features of macrophages in intermediate degeneration gland express prevailing migratory activity: **A**, macrophage extending pseudopodia (pp) into splits of the decaying syncytium. Notice residual secretory vesicles (v); **B**, this migrating macrophage exhibits bilobed nucleus, primary lysosomes (ly), and sparse complements of smooth endoplasmic reticulum (ser). The syncytial cytoplasm contains residual secretory granules (s) and empty vesicles (v); **C**, cisterns of the rough endoplasmic reticulum (rer) and primary lysosomes characterized by variable features (ly) in migrating macrophage; **D**, the same as above: notice mitochondrion with longitudinal cristae (arrow) contiguous to a bilobed nucleus, along with primary lysosomes (ly); **E**, patterns of incipient phagocytosis are also noticeable: arrow points to an "open" phagosome containing thin cytoplasm debris; **F**, details of macrophage in Fig. 2A, including open (arrow) and closed phagosomes (ph), as well as a secondary lysosome (or phagolysosome, phly).

highly variable outlines in section, according to the processes of internalization through phagosomes. When cytoplasm debris were engulfed by local invaginations of peripheral cytoplasm, macrophages exhibited plain shapes (Fig. 3E), whereas phagocytosis through repeating protrusion of laminar pseudopodia was marked by irregular cell outlines (Fig. 3F). In these macrophages involved in recurring internalization processes, merging of phagosomes with primary lysosomes gave rise to secondary lysosomes or phagolysosomes (Fig. 3F).

When macrophage activity switched into intracellular digestion of debris, re-arrangement and polarization of their substructure were observed, consisting of peripheral displacement of nuclei and formation of a wide central cytoplasm (Fig. 4A, B). Secretory syncytia undergoing phagocytosis contained minute multi-vesicular bodies (Fig. 4A), which suggested occurrence of residual activities of membrane recycling. In polarized macro-

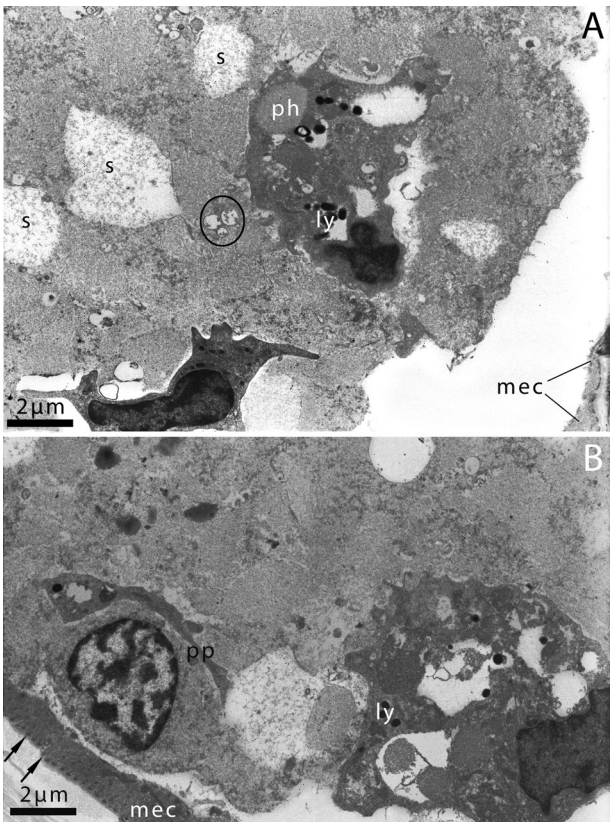

Fig. 4. The same as Fig. 3, showing differential features of macrophage activities: migration, phagocytosis, and intracellular digestion: **A**, nearby macrophages involved in migration (lower) and phagocytosis (upper), respectively. Whereas the former cell retains a high nucleus-cytoplasm ratio, the latter one displays larger cytoplasm and obvious morphological polarization, which foreshadow conversion into scavenger role: the peripheral nucleus faces a wide cytoplasm holding a phagosome (ph) and primary lysosomes (ly). The secretory syncytium, which appears to be detached from the myoepithelium (mec), contains residual secretory product (s), and multivesicular bodies (selected area). Possibly, these organelles are involved in recycling minute membrane patches that derive from merging of residual secretory granules and vesicles; **B**, along with Figs. 1A, 2A, C, this serial section fulfils a somewhat dynamic representation of phagocytosis, showing a pseudopodium (pp) that embraces the syncytial nucleus. Arrows point to hemidesmosome-like junctions on the dermal side of a slightly contracted myoepithelial cell (mec); ly, primary lysosomes.

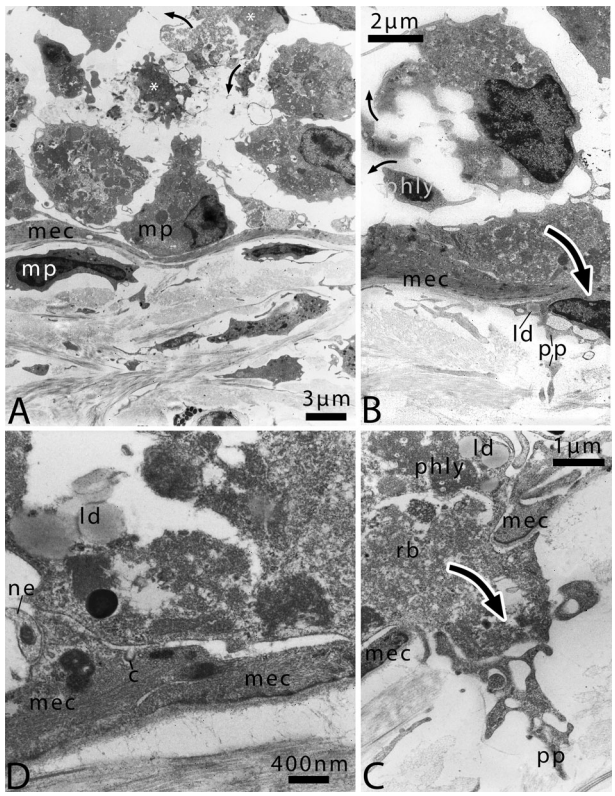

Fig. 5. TEM features of macrophages in glands undergoing ultimate stages of degeneration. The secretory syncytium has been entirely removed by scavenger macrophages, which accomplish their task transferring through reverse migration indigested residual material into the spongy dermis. However, exceeding accumulation of this material may lead to macrophage collapse: **A**, **B**, Adjacent regions of gland periphery: the large morphological variety of scavenger cells in the hollow compartment enclosed by myoepithelium (mec) contrasts the homogeneous traits of macrophages in the spongy dermis; mp, scavenger and dermal macrophages. Notice lysis of scavenger cells (*) that undergo progressive swelling and bursting out (thin bowed arrows). Large bowed arrow in panel B shows a scavenger cell coming back to the spongy dermis; ld, lipid droplet; phly, secondary lysosome or phagolysosome; pp, pseudopodium; **C**, **D**, Details of macrophages and myoepithelial cells (mec) involved in reverse migration (large bowed arrow in panel C). This scavenger cell contains lipid droplets (ld), secondary lysosomes (or phagolysosomes, phly), and residual bodies (rb). The nerve ending (ne) adjacent to myoepithelial cell, and the caveola (c) invaginating from sarcolemma do not exhibit any sign of damage, thus suggesting that advanced degeneration preserves the gland neural-contractile apparatus; pp, pseudopodium.

phages still involved in phagocytosis activity, extension of cytoplasm processes was overexpressed, when syncytium nuclei were engulfed (Fig. 4B). On the other hand, the large, central cytoplasm contained complex and extended systems of cavities, along with primary lysosomes and phagosomes (Fig. 4A, B). As expected, these macrophages were also observed in fully degenerated glands, representing continuity markers between the two stages described.

Glands in ultimate stage of degeneration. As shown in Fig. 5A, B, glands in this stage underwent integral removal of secretory unit residues. Myoepithelial cells (mecs) enclosed a hollow, electron-translucent compartment, holding the fluid remnant of the former syncytium hyaloplasm, along with a suspension of macrophages (Fig. 5A, B). These buoyant cells contained a remarkable variety of syncytium debris, and were therefore

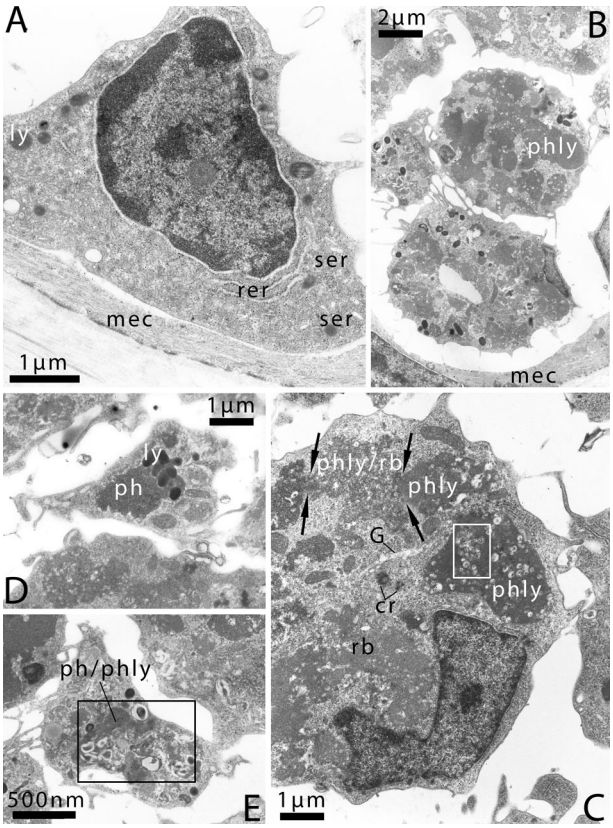

Fig. 6. The same as Fig. 5. The large morphological variety of macrophages within degenerated glands covers a wide functional array, including migratory activity and complete range of scavenger functions: from intracellular digestion to residual body assembly: **A**, this macrophage has not been yet activated for phagocytosis; it contains endoplasmic reticulum, both in the rough (rer) and smooth (ser) varieties, and primary lysosomes (ly). The myoepithelial cell (mec) exhibits a resting state, as suggested by its loose myofilament arrangement; **B**, these macrophages appear, on the contrary, differentiated as scavenger cells, and contain prominent secondary lysosomes (or phagolysosomes, phly). Notice myoepithelium (mec) enclosing the hollow compartment typical of the ultimate stage of gland degeneration; **C**, distinctive patterns of intracellular digestion are obvious in this macrophage, which exhibits a peripheral nucleus facing secondary lysosomes (or phagolysosomes, phly), residual bodies (rb), and intermediate structures between them (phly/rb). The selected area contains primary lysosome remnants "ghosts," which derive from development of phagolysosomes (compare with panel E). Arrows point to confluence between intermediate products of intracellular digestion. Also notice Golgi stack (G) and paired centrioles (cr) in the central cytoplasm; **D**, primary lysosomes (ly) merge with a dense phagosome (ph), triggering intracellular digestion; **E**, once merged, primary lysosomes release their dense content and transform into "ghost" shells (selected area, compare with panel C), giving rise to intermediate organelles (ph/phly).

referred to as scavengers, in order to emphasize their function of cytoplasmic waste removing. Due to such variable features, scavenger cells contrasted their counterpart macrophages resident in the spongy dermis, which exhibited homogeneous traits, typical of the resting and migrating phases (Fig. 5A). The wide morphological heterogeneity of scavenger features included several patterns of cytolysis, namely large, structureless and electron-transparent cytoplasm portions, as well as swellings that burst out and released their content (Fig. 5A, B). Although uncommon, such impressive features represented extreme consequences of waste accumulation in macrophage cytoplasm, which deregulated its isotonic equilibrium. However, scavenger cells loaded with remarkable amounts of waste were observed to stretch from gland to dermis (Fig. 5B). Therefore, macrophages were capable of performing reverse migratory activity through myoepithelium, despite their remarkable cargo of engulfed debris. Scavenger cells crossed the muscle sheath through gaps between contiguous myocytes, squeezing pseudopodia, followed by bulks of cytoplasm with residues of intracellular digestion (Fig. 5C). This heterogeneous waste product included subspherical inclusions (average diameter 500 nm, Fig. 5B – D) of intermediate opacity material, which resembled lipid droplets. Myocytes involved in reverse crossing showed intact functional traits (Fig. 5D): parallel arrays of thin myofilaments in sarcoplasm, pervious caveolae in sarcolemma, and adequate supply of neurites.

Fully degenerated glands also accommodated macrophages just entered from dermis, as suggested by lack of phagocytosis patterns as well as scarce cytoplasm, with organelles typical of the migrating phase (Fig. 6A): primary lysosomes and complements of the endoplasmic reticulum, consisting of flat rough cisterns arranged in parallel array, and scattered, short smooth tubules. These ser complements fitted occurrence of lipid droplets in macrophages, and denoted their capability of processing apolar molecules derived by the biochemical degradation of syncytium.

Despite the wide range of subcellular traits, the crowded central macrophages disclosed sequential patterns, which expressed steps detected in the previous stage, namely central cavities with electron-translucent compartments, numerous primary lysosomes, and complex phagolysosomes (Fig. 6B). Cells involved in early phases of debris digestion and processing exhibited a peripheral, roughly bean-shaped nucleus, its concave surface facing a wide cytoplasm with remarkable waste cargo and scanty organelles, including Golgi stacks with moderately dilated cisternae (Fig. 6C). Intracellular digestion followed a consistent functional path: primary lysosomes, gathered together and merged with phagosomes (Fig. 6D) triggering enzymatic breakdown. Primary lysosomes released their contents, and were reduced to thin shells, "ghosts," containing a structureless, low opacity core, and representing typical markers of

secondary lysosome development (Fig. 6E). However, these lysosome ghosts where still recognizable in mature secondary lysosomes that increased in size due to reciprocal merging (Fig. 6C). Confluence between secondary lysosomes in different phases of intracellular digestion, gave rise to large aggregates of heterogeneous material that underwent progressive rarefaction (Fig. 6C). Finally, undigested waste formed large residual bodies of low density, accumulating in the cytoplasm and fitting the concave nucleus surface (Fig. 6C), and were removed from the gland hollow compartment through the reverse migration of scavenger cells described above.

Subcellular traits of intercalary tract and contractile apparatus in degenerated glands. The neck region in degenerated glands maintained ordinary features in both its ultrastructure and assemblage of component cells (Fig. 7A). Intercalary stem cells shared common traits with the contiguous basal epidermal layer: high nucleus-cytoplasm ratio, as well as sparse bundles of intermediate filaments. Their ordered pile-like arrangement enclosed a slender axial interstice, the neck lumen, between gland duct (upper) and secretory unit (lower) compartments (Fig. 7A). Myoepithelial cells converged towards the intercalary tract with laminar tips, and were in turn encircled by migrating, subepidermal macrophages (Fig. 7A). Due to degeneration processes affecting secretory units, myoepithelial cells lost junctional specializations on the side facing syncytium (inner mec side), but maintained reciprocal desmosome-like apparatuses (Fig. 7B, C), except in areas involved in macrophage migration. Thin axons, provided with small dense matrix mitochondria and neurotubules, were detected while approaching the inner mec surface (Fig. 7B). Neurites reached myocytes with typical nerve endings that contained dense-cored synaptic vesicles (Fig. 7C), distinctive of an adrenergic (ortho-sympathetic) control. Near these nerve endings, mec sarcolemma formed sets of caveolae provided with an inner lining of fuzzy electron opaque material (Fig. 7B – D). These TEM features were consistent in all glands investigated, regardless of their degeneration stage, and indicated well preserved contractile apparatuses, comprehensive of myoepithelial sheath and respective supply of ortho-sympathetic neurites.

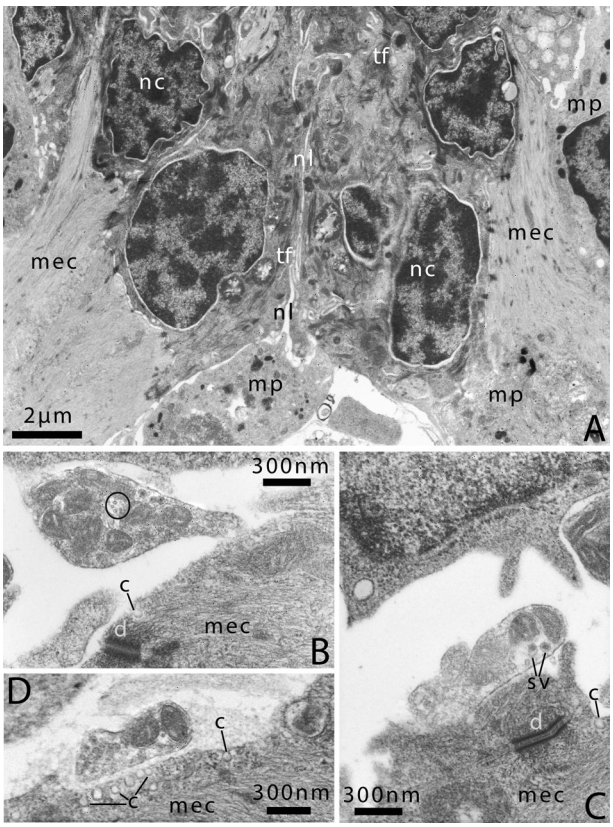

Fig. 7. TEM features of intercalated tract, or gland neck, in ultimate degeneration stage (**A**); and interstices between myoepithelium and residual syncytium in intermediate stage (**B – D**). The ultrastructural analysis of neck and neuro-contractile apparatus demonstrates their preserved state in glands undergoing collapse: **A**, stem cells in the gland neck (nc) maintain their usual piled arrangement around the slender neck lumen (nl), as well as undifferentiated ultrastructural traits, including the high nucleus-cytoplasm ratio. Notice myoepithelial cell (mec) tips converging towards the neck, and subepidermal macrophages (mp) crowding around this gland region. Notice further macrophages, differentiated as scavengers, in the gland hollow compartment. Intermediate tonofilament bundles (tf) represent the only intracytoplasmic specialised structures in neck cells; **B**, this nerve ending, which contains neurotubules (selected area), approaches myoepithelial cells (mec) joined by desmosome-like junction (d); c, caveola; **C**, nerve ending: note dense cores inside synaptic vesicles (sv), and the caveola (c) invaginating from myoepithelial cell (mec) sarcolemma; d, desmosome-like junction; **D**, numerous caveolae (c) are noticeable in this neuromuscular junction; mec, myoepithelial cell.

DISCUSSION

Despite the advanced degeneration of their secretory units, exhausted serous glands of dorsal Tungara skin can be assigned to the type Ia (Delfino et al., 2015), on the basis of common structural and ultrastructural traits. Indeed, type Ia and degenerated glands share average sizes and ellipsoidal shapes, with major axis orthogonal to parallel to the skin surface. This orientation variability is a possible adaption to fit the large secretory units of contiguous type Ib glands. Furthermore, type Ia and degenerating glands exhibit similar subcellular features in both secretory syncytia and myoepithelial envelopes. The closed profiles holding thick networks of branched microvilli correspond to the membrane-bounded cavities, which in active type Ia glands contain secretory granules of variable density, leaving wide halos around them. Microvilli

are the morphological expression of interactions between secretory granules and syncytium (Delfino et al., 2001), which enhance reciprocal transport processes during maturation (Delfino et al., 2010). Apart from limited thickenings due to local contractile responses, myoepithelial cells in degenerated glands form thin and discontinuous sheaths, with loosely arranged contractile filaments. This are also distinctive traits of type Ia myoepithelia, whereas muscle envelopes in other serous types are thick and continuous, and in Ib glands exhibit prominent spots of myofilament condensation (Delfino et al., 2015), which represent distinguishing functional features (Bani, 1976).

Present findings demonstrate that degenerated type Ia glands are massively affected by macrophages, which perform their constitutive activities: migration, phagocytosis, and intracellular digestion, and remove secretory syncytium debris completely. As a combined result of secretory unit breakdown and scavenger cell activity, degenerated glands are reduced to the mere myoepithelium. Macrophages are usual component cells of the gland stroma (the spongy dermis), and in tadpoles extend their patrolling range to epidermis (Delfino et al., 2014, Fig. 2E). These migrating cells respond to stresses affecting serous glands, including infestations by nematodes. Round worms penetrate into the gland through the continuous lumina of duct and intercalary tract, and are hosted in special chambers continuous with the exiguous lumen of the secretory unit (Sevinc et al., 2005). Although nematodes evoke an impressive immune response, the syncytium of glands undergoing verminous infestation keeps its integrity, and limits progression of migrating cells to the interstice between myoepithelium and secretory unit. In degenerating glands the syncytium leaves this structural stiffness and is integrally penetrated by macrophages

Usually, degeneration of the secretory syncytium occurs following gland depletion induced by myoepithelium contraction, which squeezes granules as well parts of the cytoplasm storing them onto skin surface. This is a phasic and massive holocrine process (bulk discharge), which contrasts with the tonic, merocrine release (Delfino et al., 1996; 2014). Bulk discharge is usually induced through epinephrine in studies of functional anatomy of anuran serous glands, which mimic the ortho-sympathetic control of mecs (Delfino, 1980, 1990; Delfino et al., 1982, 2002, 2006; Barberio et al., 1987; Mastromei et al., 1991; Balboni et al., 1992; Sanna et al., 1993; Nosi et al., 2002; Quagliata et al., 2008b; Melzer et al., 2013). This experimental method has been pioneered by Faraggiana (1938, 1939), who firstly described macrophage recruitment after gland depletion. TEM investigations of depleted glands fully confirmed such innovative approach: macrophages, usually present in the syncytium/myoepithelium interstices (Delfino et al., 1992, 1998), penetrate the secretory unit and are recognizable between residual granules and cytoplasm remnants (Nosi et al., 2002).

Although bulk depletion induces structural and ultrastructural changes resembling features described in the present report, the differential analysis discloses contrasting traits. Degenerating glands in Tungara exhibit the usual ellipsoidal shape, whereas glands depleted experimentally look like headache ice packs (Nosi et al., 2002; Quagliata et al., 2008b), due to contraction of the spindle-like mecs arranged according to meridian planes (Bani, 1976). Possibly, the remarkable crowd of internal macrophages and the fluid medium residual from syncytium collapse, contribute to shape stability, opposing eventual local contractions of mecs. Indeed, myoepithelium in degenerated glands of Tungara displays usual ultrastructural features, whereas contracted mecs in glands depleted by bulk discharge exhibit reshaping of their external surface, displacement of organelles and thickening of the myofilament array (Delfino, 1991: Fig. 3D; Delfino et al., 2006).

Once excluded that gland degeneration in Tungara results from forced depletion, a suitable hypothesis of secretory syncytium decay stems from peculiar functional traits displayed by type Ia secretory units during granule storage and maturation, in comparison with type Ib (Delfino et al., 2015). Type Ia glands exhibit a double functional polarization: periphery-center and center-periphery. Central granules undergo partial disintegration during storage, whereas the peripheral ones are expelled into the mec-syncytium interstice by means of merocrine release. Regulative molecules of the secretory product may then diffuse into the spongy dermis through wide gaps between mecs, and reach stromal targets, performing a paracrine role. In comparison, type Ib granules undergo a marked condensation, namely a phase transition that allows storing noxious molecules within suitable protein scaffoldings (Nosi et al., 2013). In addition, type Ib glands contain peculiar autophagosomes, possibly related to the process of crinophagy (Glaumann, 1989), which regulates intra-cytoplasmic storage of noxious molecules in anuran serous glands (Delfino et al., 1999; Arifulova et al., 2007). Type Ia glands of Tungara exploit neither maturational condensation nor crinophagy, but appear to be involved in steady stage equilibrium between secretory neosynthesis/storage and merocrine release of secretory granules. Deregulation of such dynamic equilibrium leads to potentially noxious over-storage of secretory products and byproducts in the cytoplasm. In the absence of adequate control of accumulation of harmful molecules through crinophagy, the syncy-

tium undergoes degeneration. This peculiar apoptotic process allows macrophages to gain access to the gland interior via the pathway generated by syncytium collapse. In addition, degradation of cytoplasm produces signal molecules that orientate cell migration as well as protrusion of pseudopodia in preparation of bulk phagocytosis.

Finally, scavenger activity of macrophages appears to be topographically selective, since their molecular targeting involves only the syncytium, whereas it spares other fundamental regions of the gland: intercalated tract and neural-contractile apparatus, which do not display any degeneration hallmark. In this respect, it appears noteworthy the conservation of feeble plasma membrane specializations, such as mec caveolae in degenerated glands. These microdomains of sarcolemma, described in mecs of various exocrine glands of vertebrates (Sopel, 2010), are common in smooth muscle cells, where they play a fundamental role in coupling neural/hormonal to contractile/transductional events (Popescu et al., 2006). Therefore, a selective mechanism of turnover, based on proliferation and cytodifferentiation of neck stem cells (Delfino, 1980; Quagliata et al., 2008b), may generate a new secretory unit, which grows into the hollow space bounded by myoepithelium and may rely on its intact neural-contractile apparatus to restore full functional gland rehabilitation.

REFERENCES

Arifulova I., Delfino G., Dujsebayeva T., Fedotovskikh G., Nosi D., and Terreni A. (2007), "Serous cutaneous glands in the South American horned frog *Ceratophrys ornata* (Leptodactylformes, Chthonobatrachia, Ceratophrydae): Ultrastructural expression of poison biosynthesis and maturation," *J. Morphol.*, **268**, 690 – 700.

Balboni F., Bernabei P. A., Barberio C., Sanna A., Rossi Ferrini P. G., and Delfino G. (1992), "Cutaneous venom of *Bombina variegata pachypus* (Amphibia, Anura): effects on the growth of the human HL 60 cell line," *Cell Biol. Int. Rep.*, **16**, 329 – 338.

Bani G. (1976), "Cellule mioepiteliali accluse alle ghiandole cutanee di alcuni Anfibi," *Archo Ital. Anat. Embriol.*, **81**, 133 – 184.

Barberio C., Delfino G., and Mastromei G. (1987), "A low molecular weight protein with antimicrobial activity in the cutaneous 'venom' of the yellow-bellied toad (*Bombina variegata pachypus*)," *Toxicon*, **25**, 899 – 909.

Delfino G. (1980), "L'attività rigeneratrice del tratto intercalare nelle ghiandole granulose cutanee dell'Ululone *Bombina variegata pachypus* (Bonaparte) (Anfibio, Anuro, Discoglosside); studio sperimentale al microscopio elettronico," *Archo Ital. Anat. Embriol.*, **85**, 283 – 310.

Delfino G. (1991), "Ultrastructural aspects of venom secretion in anuran cutaneous glands," in: A. T. Tu (ed.), *Handbook of Natural Toxins. Vol. 5. Reptile and Amphibian Venoms*, Marcel Dekker Inc., New York, pp. 777 – 801.

Delfino G., Amerini S. and Mugelli A. (1982), "In vitro studies on the 'venom' emission from the skin of *Bombina variegata pachypus* (Bonaparte) (Amphibia Anura Discoglossidae)," *Cell Biol. Int. Rep.*, **6**, 843 – 850.

Delfino G., Brizzi R., Alvarez B. B., and Kracke-Berndorff R. (1998), "Serous cutaneous glands in *Phyllomedusa hypochondrialis* (Anura, Hylidae): secretory patterns during ontogenesis," *Tissue Cell*, **30**, 30 – 40.

Delfino G., Brizzi R., Alvarez B. B., and Gentili M. (1999), "Granular cutaneous glands in the frog *Physalaemus biligonigerus* (Anura, Leptodactylidae): a comparison between ordinary serous and "inguinal" glands," *Tissue Cell*, **31**, 576 – 586.

Delfino G., Brizzi R., and Borrelli G. (1988), "Cutaneous glands in Anurans: Differentiation of the secretory syncytium in serous anlagen," *Zool. Jb. Anat.*, **117**, 255 – 275.

Delfino G., Brizzi R., and Calloni C. (1990), "A morphofunctional characterization of the serous cutaneous glands in *Bombina orientalis* (Anura: Discoglossidae)," *Zool. Anz.*, **225**, 295 – 310.

Delfino G., Brizzi R., De Santis R., and Melosi M. (1992), "Serous cutaneous glands of the western spade-foot *Pelobates cultripes* (Amphibia: Anura): an ultrastructural study on adults and juveniles," *Archo Ital. Anat. Embriol.*, **97**, 109 – 120.

Delfino G., Brizzi R., and Melis G. (1996), "Merocrine secretion from serous cutaneous glands in *Rana esculenta* complex and *Rana iberica*," *Alytes*, **13**, 179 – 192.

Delfino G., Brizzi R., Nosi D., and Terreni A. (2002), "Serous cutaneous glands in New World hylid frogs: an ultrastructural study on skin poisons confirms phylogenetic relationships between *Osteopilus septentrionalis* and *Phrynohyas venulosa*," *J. Morphol.*, **253**, 176 – 186.

Delfino G., Drewes R. C., Magherini C., Malentacchi C., Nosi D. and Terreni A. (2006), "Serous cutaneous glands of the Pacific tree-frog *Hyla regilla* (Anura, Hylidae): Patterns of secretory release induced by nor-epinephrine," *Tissue Cell*, **38**, 65 – 77.

Delfino G., Giachi F., Malentacchi C., and Nosi D. (2015), "Ultrastructural evidence of serous gland polymorphism in the skin of the tungara frog *Engystomops pustulosus* (Anura Leptodactylidae)," *The Anat. Rec.*, **298**, 1659 – 1667.

Delfino G., Giachi F., Nosi D., and Malentacchi C. (2010), "Serous cutaneous glands in *Phyllobates bicolor* (Anura: Dendrobatidae): an ontogenetic, ultrastructural study on secretory product biosynthesis and maturation," *Copeia*, **2010**, 27 – 37.

Delfino G., Giachi F., and Nosi D. (2014), "Poison storage and maturation in serous cutaneous glands of anurans: an integrative ultrastructural outlook," in: H. Lambert (ed.), *Frogs: Genetic Diversity, Neural Development and Ecological Implication*, Nova Publishers, New York, pp. 1 – 71.

Delfino G., Nosi D., and Giachi F. (2001), "Secretory granule-cytoplasm relationships in serous glands of anurans: ultra-

structural evidence and possible functional role," *Toxicon*, **39**, 1161 – 1171.

Faraggiana R. (1938), "Ricerche istologiche sulle ghiandole cutanee granulose degli Anfibi Anuri. I. *Bufo vulgaris* e *Bufo viridis*," *Archo Ital. Anat. Embriol.*, **39**, 327 – 376.

Faraggiana R. (1939), "Ricerche istologiche sulle ghiandole cutanee granulose degli Anfibi Anuri. II. *Rana esculenta*, *Rana agilis* e *Bombinator pachypus*," *Archo Ital. Anat. Embriol.*, **41**, 390 – 410.

Glaumann H. (1989), "Crinophagy as a means for degrading excess secretory proteins in rat liver," *Rev. sobre Biol. Celular*, **20**, 97 – 110.

Karnovsky M. J. (1965), "A formaldehyde-glularaldehyde fixative of high osomolarity for use in electron microscopy," *J. Cell Biol.*, **27**, 137A.

Mastromei G., Barberio C., Pistolesi S., and Delfino G. (1991), "A bactericidal protein in *Bombina variegata pachypus* skin venom," *Toxicon*, **29**, 321 – 328.

Melzer S., Clerens S., and Bishop P. J. (2013), "Skin gland morphology and secretory peptides in naturalized *Litoria* species in New Zealand," *J. Herpetol.*, **47**, 565 – 574.

Nosi D., Delfino G., and Quercioli F. (2013), "Serous cutaneous glands in anurans: Fourier transform analysis of the repeating secretory granule substructure," *Naturwissenschaften*, **100**, 209 – 218.

Nosi D., Terreni A., Alvarez B. B., and Delfino G. (2002), "Serous cutaneous gland polymorphism in the skin of *Phyllomedusa hypochondrialis azurea* (Anura, Hylidae). Response by different gland types to norepinephrine stimulation," *Zoomorphology*, **121**, 139 – 148.

Popescu L. M., Gherghiceanu M., Mandache E., and Cretoiu D. (2006), "Caveolae in smooth muscles: nanocontacts," *J. Cell. Mol. Med.*, **10**, 960 – 990.

Quagliata S., Malentacchi C., Giachi F., and Delfino G. (2008b), "Chemical skin defence in the Eastern fire-bellied toad *Bombina orientalis*: an ultrastructural approach to the mechanism of poison gland rehabilitation after discharge," *Acta Herpetol.*, **3**, 139 – 153.

Quagliata S., Pacini S., Punzi T., Malentacchi C., Ruggiero M., and Delfino G. (2008a), "Bombesin promotes vasculogenesis and angiogenesis in chick chorio-allantoic membrane: a morphometric, structural and ultrastructural study," *J. Morphol.*, **269**, 72 – 83.

Sanna A., Bernabei P. A., Rossi Ferrini P., Brunelli T., and Delfino G. (1993), "The cutaneous venom of *Bombina orientalis*: cytotoxic effects on the human HL 60 cell line and a comparison with *Bombina variegata*," *J. Nat. Toxins*, **2**, 161 – 173.

Sevinc M., Nosi D., Brizzi R., Terreni A., Malentacchi C., and Delfino G. (2005), "Ultrastructural study on host-guest relationships between anuran serous cutaneous glands and nematodes," *Caryologia*, **58**, 112 – 131.

Sopel M. (2010), "The myoepithelial cell: its role in normal mammary glands and breast cancer," *Folia Morphol.*, **69**, 1 – 14.